Supporting Information

Cheah et al. 10.1073/pnas.1424795112

SI Materials and Methods

Mice and Cell Lines. All animal procedures were approved by the International Animal Care and Use Committee and the Stanford University Administrative Panel on Laboratory Animal Care. C57BL/6, C57BL/6 Rosa26-mRFP1, C57BL/6 RAG$^{-/-}\gamma_c^{-/-}$, and NOD.Cg-Prkdc^{scid} Il2rg^{tm1Wjl}/SzJ (NSG) mice were derived and maintained at Stanford University. The tumor cell line 639V (human bladder cancer) was cultured at 37 °C and 5% (vol/vol) CO_2 in Eagle's Minimum Essential Medium (American Type Culture Collection) supplemented with 10% (vol/vol) FCS, 100 μg/mL penicillin, and 100 μg/mL streptomycin. The tumor cell line MB49 (mouse bladder cancer) was induced by 7, 12-di-methylbenzanthrene. MB49 was cultured at 37 °C and 5% (vol/vol) CO_2 in DMEM supplemented with 10% FCS, 1% L-glutamine, 100 μg/mL penicillin, and 100 μg/mL streptomycin.

Identification of Surface Markers Enriched on KRT14+ Patient BC Samples. Surface markers enriched on KRT14+ patient BC samples were predicted using Hegemon as previously described (1).

Bladder Tumor Tissue Dissociation. Tumor tissues were mechanically dissociated in Medium 199 containing Liberase TM and TH enzymes (Roche) and DNase (Worthington) at 37 °C until single-cell suspension was achieved (1–3 h). Cells were then washed twice with PBS and filtered through a 100-μm filter.

Flow Cytometry Analysis and Cell Sorting. Human tumor cell suspensions and 639V were stained with PE/Cy7-conjugated anti-CD14 (Biolegend; 325618), FITC-conjugated anti-CD90 (Biolegend; 328108), PerCP/Cy5.5-conjugated anti-ESA (Biolegend; 324214), and lineage mixture containing Pacific-blue–conjugated anti-CD45 (Biolegend; human 304022 and mouse 103125), anti-CD31 (Biolegend; human 303114 and mouse 102422), and anti-H-2Kd (Biolegend; 116616) antibodies with DAPI as a live/dead stain. Flow cytometry analysis and cell sorting was performed on a BD FACSAria (Becton Dickinson) cell sorting system under 20 psi with a 100-μm nozzle as previously described (1). To purify subpopulations of 639V cells, CD14-high and -low cells were isolated from bulk 639V via FACS followed by in vitro culture. Serial FACS and in vitro culture was repeated seven times. Mouse MB49 cells were stained with allophycocyanin (APC)-conjugated anti-CD14 (Biolegend; 123312) and PE-conjugated anti-CD44 (Biolegend; 103024). To purify subpopulations of MB49 cells, CD14-high and -low cells were isolated from bulk MB49 via FACS followed by in vitro culture. Serial FACS and in vitro culture was repeated 10 times. For tumor composition analysis, tumor cell suspensions were stained with FITC-conjugated anti-CD31 (Biolegend; 102506), PE-conjugated anti-I-A^b (Biolegend; 116408), PerCP/Cy5.5-conjugated anti-CD11b (Biolegend; 101228), PE/Cy7-conjugated anti-F4/80 (Biolegend; 123114), APC-conjugated anti-CD45 (Biolegend; 103112), APC/Cy7-conjugated anti-Gr-1 (Biolegend; 108424), Brilliant Violet 421-conjugated anti-CD11c (Biolegend; 301628) with propidium iodide as a live/dead stain. For macrophage polarization analysis, tumor cell suspensions were stained with Alexa Fluor 488-conjugated anti-CD301 (AbD Serotec; MCS2392A488) and Alexa Fluor 647-conjugated anti-CD206 (Biolegend; 321116). For T-cell analysis, tumor cell suspensions were stained with PE-conjugated anti-CD4 (Biolegend; 100408), PerCP/Cy5.5-conjugated anti-CD8α (Biolegend; 100734), PE/Cy7-conjugated anti-CD3ε (Biolegend; 100320), and APC/Cy7-conjugated anti-CD90.1 and CD90.2 (Biolegend; 202520 and 105328).

Immunofluorescence Staining. Optimal cutting temperature compound-embedded frozen tissue was sectioned into 5-μm thick sections and fixed with ethanol. Slides were then blocked with 10% (vol/vol) goat serum and probed with anti-CD14 (Biolegend; 325618), anti-EpCAM (Abcam; ab71916), or anti-CD31 (BD; 553372) antibodies overnight at 4 °C. Samples were stained with goat anti-mouse and anti-rabbit secondary antibodies conjugated with Alexa 488/594 (Invitrogen) and nuclear-counterstained with Hoechst (Invitrogen). Slides were imaged on a Leica fluorescent microscope.

Real-Time PCR. Total RNA was isolated from sorted cell populations using the RNeasy Plus Micro kit (Qiagen) according to the manufacturer's protocol. RNA was then subjected to cDNA synthesis using superscript III (Invitrogen) according to the manufacturer's protocol. The cDNA was then run on an ABI 7900 machine with Taqman probe PCR reactions (Applied Biosystems) according to the manufacturer's protocol. The qPCR results were normalized using β-actin as endogenous control (Hu-β-actin, Hs00357333_g1; KRT14, Hs00559328_m1; Hu-CD14, Hs02621496_s1; IL6, Hs00985639_m1; IL8, Hs00174103_m1; Csf1, Hs00174164_m1; Fgf2, Hs00266645_m1; Vegfa, Hs00900055_m1; Ms-β-actin, Mm00607939_s1; Ms-CD14, Mm00438094_g1; Applied Biosystems).

Cell Line Culture. CM from 639V and MB49 cells are produced as described below. Briefly, cells were plated at a density of 200,000 cells/well in a 48-well plate with a media volume of 200 μL/well. Supernatants were collected 24 h after plating. Cultures were scaled-up as necessary. Tumor CM was filtered through a 0.22-μm Millipore filter to remove cell debris before use in subsequent experiments.

Luminex. Human 51-plex or mouse 26-plex kits were purchased from Affymetrix and used according to the manufacturer's recommendations with modifications as described below. Briefly, samples were mixed with antibody-linked polystyrene beads on 96-well filter-bottom plates and incubated at room temperature for 2 h followed by overnight incubation at 4 °C. Plates were vacuum-filtered and washed twice with wash buffer and then incubated with biotinylated detection antibody for 2 h at room temperature. Samples were then filtered and washed twice as above and resuspended in streptavidin–PE. After incubation for 40 min at room temperature, two additional vacuum washes were performed, and the samples were resuspended in Reading buffer. Each sample was measured in duplicate. Plates were read using a Luminex 200 instrument with a lower bound of 100 beads per sample per cytokine.

Quantification of Soluble Factors. Human IL6 and IL8 and mouse IL6, CCL3, CXCL1, CXCL2, CXCL5, G-CSF, and LIF enzyme-linked immunoabsorbent assay (ELISA) kits were from R&D Systems. Nitric oxide quantification kit was from R&D Systems (KGE001). Prostaglandin E2 quantification kit was from Cayman Chemical Company (500141). Concentration of soluble factors was quantitated according to the manufacturer's instructions (hIL6, DY206; IL8, DY208; mIL6, DY406; CCL3, DY450; CXCL1, DY453; CXCL2, DY452; CXCL5, DY443; G-CSF, DY414; LIF, MLF00).

Microarray Analysis of BC Cell Lines. We performed microarrays on CD14-high and -low cells. RNA was isolated with RNeasy Micro Kit (Qiagen) per the manufacturer's instructions from three

independent samples. mRNA amplification was performed using a two-cycle target-labeling system for 3′ in vitro transcription, hybridized to a mouse genome 430 2.0 array, and scanned according to the manufacturer's protocol (Affymetrix). Background correction and signal normalization was performed using the standard multichip average algorithm (2, 3). Analysis was conducted using GSEA and Gene Expression Commons (4).

Tumor Cell Engraftment. Tumor cells were suspended with 50% Matrix-Matrigel (Becton Dickinson; 354248) in Medium M199 and injected (MB49: 1.0×10^5 cells, 639V: 2.5×10^5 cells), as indicated, s.c. into the dorsal skin of 6- to 8-wk-old C56BL/6, C57BL/6 RAG$^{-/-}$ $\gamma_c^{-/-}$, or NOD.Cg-Prkdc^{scid} Il2rg^{tm1Wjl}/SzJ (NSG) mice. After 4 wk (MB49) or 8 wk (639V), tumors were resected and weighed.

Immune Cell Isolation and Culture. Immune cells (T cells and myeloid cell subsets) were cultured at 37 °C and 5% (vol/vol) CO_2 in RPMI supplemented with 10% (vol/vol) FCS, 1% L-glutamine, 55 μM 2-mercaptoethanol, 1 mM sodium pyruvate, 100 μg/mL penicillin and 100 μg/mL streptomycin. Macrophage, monocyte, neutrophils, and DCs were generated from C57BL/6 Rosa26-mRFP1 mice. Monocytes and neutrophils were isolated from mouse bone marrow using an EasySep mouse monocyte enrichment kit (19761) and an EasySep mouse neutrophil enrichment kit (19762), respectively, according to manufacturer's instructions. To obtain DCs, bone-marrow–derived monocytes were cultured in RPMI supplemented with 20 ng/mL GM-CSF and IL4 for 7 d. To obtain macrophages, bone marrow cells were cultured in RPMI supplemented with 20 ng/mL M-CSF for 7 d. To obtain tumor CM-differentiated monocytes, bone-marrow–derived monocytes were cultured in 50% (vol/vol) CD14-high or CD14-low tumor CM in RPMI for 7 d. To obtain differentially polarized macrophages, bone-marrow–derived macrophages were prepared and harvested and further cultured in RPMI supplemented with 60 ng/mL IFNγ (M1), 20 ng/mL IL4, and IL10 (M2) or 50% (vol/vol) tumor CM in RPMI (tumor macrophage) for 2 more days. All cytokines were purchased from Peprotech (GM-CSF, 315–03; M-CSF, 315–02; IFNγ, 315–05; IL4, 214–14; IL10, 210–10).

Cell Migration Assay. Polystyrene plates (24-well) with polycarbonate membranes separating the upper and lower wells in a transwell chamber system (Corning) were used. A 5-μm pore size was used for monocytes and neutrophils, and a 8-μm pore size was used for macrophages and DCs. The bottom wells of the chamber were filled with 50% CM in RPMI, and 1×10^5 myeloid cells cultured in RPMI were added to the upper chamber. The transwell chamber was incubated at 37 °C for 24 h to allow the migration of cells through the membrane into the lower chamber. The migrated cells were stained with trypan blue and counted with a hemacytometer.

T-Cell Activation Assay. For in vitro T-cell activation assays, 1×10^4 of the indicated APCs (macrophage or monocyte subsets) was pulsed with 10 μM of OT-I peptide (OVA 257–264; SIINFEKL) or OT-II peptide (OVA 323–339; ISQAVHAAHAEINEAGR) for 4 h, and excess peptide was washed away. Peripheral lymph nodes and spleens were harvested from OT-I or OT-II TCR transgenic mice and labeled with 0.5 mM carboxyfluorescein diacetate, succinimidyl ester (CFSE) (Molecular Probes). T cells were isolated using anti-CD8 or anti-CD4 magnetic beads (Miltenyi Biotec). Then 5×10^4 T cells were added to the cultures and analyzed on day 3 (for OT-I T cells) or day 4 (for OT-II T cells).

Quantification of Nitric Oxide Concentration and Arginase Activity. Bone-marrow–derived macrophage subsets were generated as described above and stimulated with 10 μg/mL LPS (InvivoGen; tlrl-eklps) for 24 h. Supernatants were harvested and filtered through a 0.22-μm Millipore filter, and nitric oxide concentrations were determined as described above. LPS-stimulated macrophages were harvested and arginase activities of macrophage subsets were quantitated with the Arginase Assay Kit (Abnova; KA1609) according to the manufacturer's instructions.

Tumor Cell Proliferation Assay. Proliferation rates of tumor cell subsets were determined with the BrdU Cell Proliferation Assay Kit (Cell Signaling Technology; 6813) according to the manufacturer's instructions using a starting cell density of 3×10^4 cells/well in a 96-well plate. For assays in exogenously added CM, cells were cultured in 50% (vol/vol) of the respective CMs mixed with DMEM.

TALEN Design and Construction. TALENs were designed and assembled as described (5). The ORF of mouse *CD14* (×13,987.1) was scanned for putative TALEN-binding pairs. The pairs TGCTTCTGGTGCACGCCTCT and TTCCTCGTCTAGCTCGCAGG, respectively, were cloned into the pTALEN backbone.

TALEN Transfection and Sorting. CD14-high MB49 cells were grown in DMEM as described above. Transfection of the plasmids expressing the *CD14* TALEN pair into CD14-high MB49 cells was performed using TransIT-2020 Transfection Reagent (Mirus) in six-well tissue culture plates according to manufacturer instructions. The cells were collected from the culture plates 96 h posttransfection using TrypLE (Life Technologies) and stained with APC-conjugated anti-CD14 (Biolegend; 123312). Cells that were CD14-negative were isolated by FACS sorting.

Blocking of CD14, TLRs, and TLR Adaptor Molecules. CD14-high MB49 cells were pretreated for 24 h with control (isotype antibody or DMSO) or with the indicated inhibitor. Cell supernatants were replaced, and cells were further treated for another 24 h before supernatant collection and ELISA to determine changes in IL6 production [CD14 MAb (BD), 557896, 10 μg/mL; OxPAPC (InvivoGen), tlrl-oxp1, 30 μg/mL; TLR4 MAb (InvivoGen), mab-mtlr4md2, 10 μg/mL; TLR2 MAb, (InvivoGen), mabg-mtlr2, 1 μg/mL; MyD88 Inhibitory Peptide (InvivoGen), tlrl-pimyd, 50 μM; TIRAP Inhibitory Peptide (Imgenex), IMG-2006–1, 25 μM; TRIF Inhibitory Peptide (InvivoGen), tlrl-pitrif, 10 μM]. For experiments involving choloroquine, CD14-high MB49 cells were pretreated for 4 h with chloroquine, and cell supernatants were replaced. Cells were further treated with chloroquine for another 4 h before supernatant collection and ELISA to determine changes in IL6 production.

Statistical Analysis. The *t* test was applied to all comparisons of mean values. All statistical analyses were performed on Prism 6 software (GraphPad).

1. Volkmer JP, et al. (2012) Three differentiation states risk-stratify bladder cancer into distinct subtypes. *Proc Natl Acad Sci USA* 109(6):2078–2083.
2. Inlay MA, et al. (2009) Ly6d marks the earliest stage of B-cell specification and identifies the branchpoint between B-cell and T-cell development. *Genes Dev* 23(20):2376–2381.
3. Sahoo D, et al. (2010) MiDReG: A method of mining developmentally regulated genes using Boolean implications. *Proc Natl Acad Sci USA* 107(13):5732–5737.
4. Seita J, et al. (2012) Gene Expression Commons: An open platform for absolute gene expression profiling. *PLoS ONE* 7(7):e40321.
5. Sanjana NE, et al. (2012) A transcription activator-like effector toolbox for genome engineering. *Nat Protoc* 7(1):171–192.

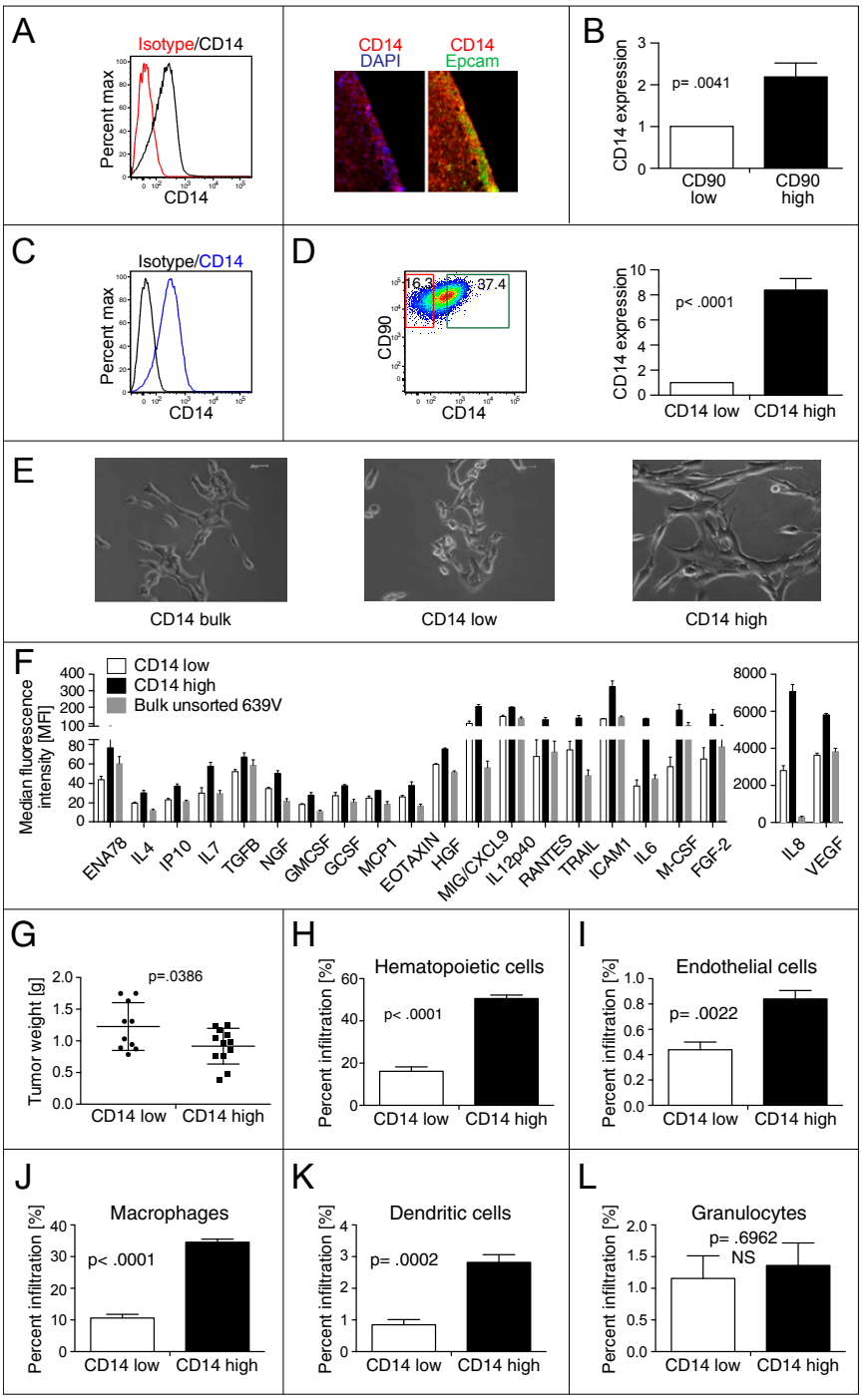

Fig. S1. BC contains CD14-expressing cells that produce inflammatory factors. (*A*, *Left*) Representative flow cytometry analysis of basal patient BC samples. Tumor cells shown were gated for lineage (CD31, H-2Kd, CD45)-negative live cells. Tumor cells stained with anti-CD14 antibody is compared with isotype control. (*Right*) Immunofluorescence staining of CD14 and EpCAM in primary BC samples. (*B*) qPCR of CD14 mRNA in CD90– and CD90+ tumor cells from basal patient BC samples ($n = 3$). Tumor cells were gated based on live, lineage (CD45, CD31)-negative cells (mean and SEM; $P = 0.0041$). (*C*) Representative flow cytometry analysis of human BC cell line 639V. Tumor cells stained with anti-CD14 antibody are compared with isotype control. (*D*, *Left*) Serial FACS isolation of CD14-low and CD14-high subpopulations from bulk 639V tumor cells. (*Right*) qPCR of CD14 mRNA in each subpopulation ($n = 4$) (mean and SEM; $P < 0.0001$). (*E*) Bright-field microscopy images showing the morphology of each 639V subpopulation. (*F*) Cytokine profiling of CD14-low, CD14-high, and bulk-unsorted 639V cells using Luminex arrays ($n = 4$). *P* value is analyzed for difference in cytokine production between CD14-high and -low cells (mean and SEM; ENA78, $P = 0.0029$; IL4, $P = 0.0018$; IP10, $P < 0.0001$; IL7, $P = 0.0013$; TGFβ, $P = 0.0074$; NGF, $P = 0.0025$; GM-CSF, $P = 0.0130$; G-CSF, $P = 0.0226$; MCP1, $P = 0.0099$; Eotaxin, $P = 0.0262$; HGF, $P < 0.0001$; MIG, $P = 0.0019$; IL12p40, $P = 0.0004$; RANTES, $P = 0.0194$; TRAIL, $P = 0.0131$; ICAM1, $P = 0.0013$; IL6, $P < 0.0001$; IL8, $P < 0.0001$; M-CSF, $P = 0.0130$; VEGF, $P < 0.0001$; FGF-2, $P = 0.0184$). (*G*) Growth of ectopic tumors formed by s.c. injection of CD14-low ($n = 10$) and CD14-high ($n = 12$) 639V human BC subpopulations into immunocompromised NSG mice after 8 wk (mean and SEM; $P = 0.0386$). (*H* and *I*) Frequencies of total hematopoietic cell (CD45+) and endothelial cell (CD31+) infiltration in tumors formed by CD14-low and CD14-high 639V subpopulations by flow cytometry ($n = 5$). Cell frequencies were calculated based on percentage of the indicated cell population over total live cells (mean and SEM; Hematopoietic cells, $P < 0.0001$; Endothelial cells,

Legend continued on following page

$P = 0.0022$). (*J–L*) Frequencies of myeloid cell infiltration in tumors formed by CD14-low and CD14-high 639V subpopulations in immune-compromised NSG mice by flow cytometry. Myeloid cells were gated based on expression of CD45. Cell frequencies were calculated based on percentage of the indicated cell population over total live cells ($n = 5$). Macrophages/monocytes (CD11b+ F4/80+); DCs (CD11b+ CD11c+); Granulocytes (CD11b− Gr1+) (mean and SEM; Macrophages/monocytes, $P < 0.0001$; DCs, $P = 0.0002$; Granulocytes, $P = 0.6962$, not significant).

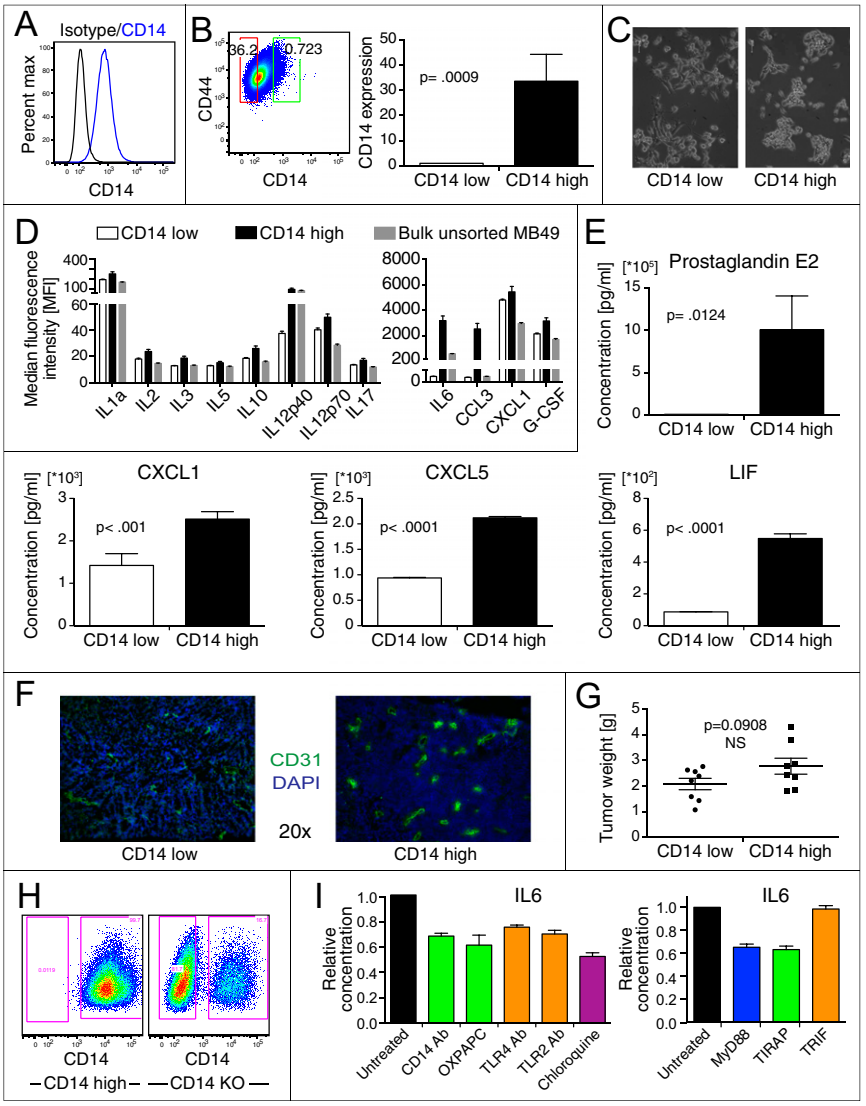

Fig. S2. CD14 expression on BC cells promotes inflammatory cytokine production and tumor growth. (*A*) Representative flow cytometry analysis of mouse BC cell line MB49. Tumor cells stained with anti-CD14 antibody are compared with isotype control. (*B*, *Left*) Serial FACS isolation of CD14-low and CD14-high subpopulations from bulk MB49 tumor cells. (*Right*) qPCR of CD14 mRNA in each subpopulation ($n = 4$) (mean and SEM; $P = 0.0009$). (*C*) Bright-field microscopy images showing the morphology of each MB49 subpopulation. (*D*) Cytokine profiling of CD14-low, CD14-high, and bulk-unsorted MB49 cells using Luminex arrays ($n = 6$). *P* value is analyzed for difference in cytokine production between CD14-high and -low cells (mean and SEM; IL1a, $P = 0.0263$; IL2, $P = 0.0082$; IL3, $P = 0.0026$; IL5, $P = 0.0409$; IL10, $P = 0.0037$; IL12p40, $P = 0.0005$; IL12p70, $P = 0.0071$; IL17, $P = 0.0418$; IL6, $P < 0.0001$; CCL3, $P = 0.0002$; G-CSF, $P = 0.0025$). (*E*) Differences in inflammatory small-molecule, cytokine, and chemokine production between CD14-low and CD14-high mouse BC cells measured by ELISA (mean and SEM; PGE_2, $P = 0.0124$; CXCL5, $P < 0.0001$; CXCL1, $P < 0.0001$; LIF, $P < 0.0001$). (*F*) Immunofluorescence staining of CD31 in tumors formed by MB49 mouse BC subpopulations. Green cells forming vessel-like structures represent tumor vasculature. (*G*) Growth of ectopic tumors formed by s.c. injection of CD14-low and CD14-high MB49 mouse BC subpopulations into immune-compromised $RAG^{-/-}\ \gamma_c^{-/-}$ C57BL/6 mice ($n = 8$) after 4 wk (mean and SEM; $P = 0.0908$, not significant). (*H*) FACS isolation of CD14-high MB49 cells transfected with TALEN specific for CD14 (CD14 KO). (*I*) IL6 production by CD14-high MB49 cells when treated with a series of blocking antibodies, compounds, and inhibitory peptides that target different components of TLR signaling ($n = 3$). *P* value is analyzed for difference in cytokine production between treated and untreated cells (mean and SEM; CD14 MAb, $P = 0.0002$; OxPAPC, $P = 0.0085$; TLR4 MAb, $P = 0.0001$; TLR2 MAb, $P = 0.0005$; Chloroquine, $P < 0.0001$; MyD88, $P = 0.0002$; TIRAP, $P = 0.0003$; TRIF, $P = 0.6273$, not significant).

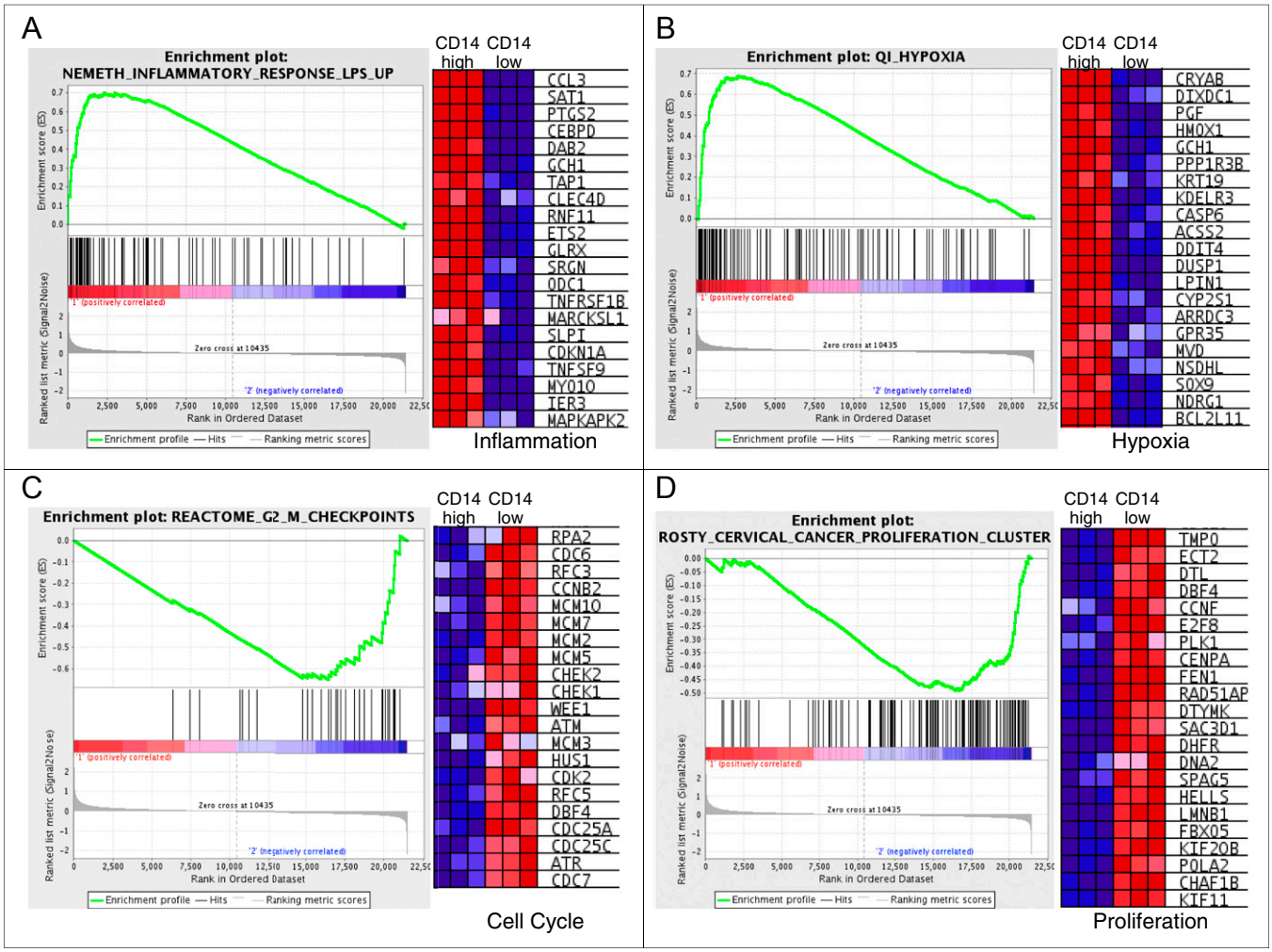

Fig. S3. CD14-high cells express genes that are associated with inflammation and hypoxia, whereas CD14-low cells express genes that are associated with cell cycle regulation and cell proliferation. Gene set enrichment analysis of CD14-high cells revealed an association with genes up-regulated in RAW 264.7 cell macrophages 3 h after stimulation with LPS (*A*) and genes up-regulated by TRAMP-C prostate cancer cells during hypoxia (*B*). Gene set enrichment analysis of CD14-low cells revealed an association with genes involved in the G2/M checkpoint of the cell cycle (*C*) and genes corresponding to the E2F pathway controlling cell division or proliferation (*D*).

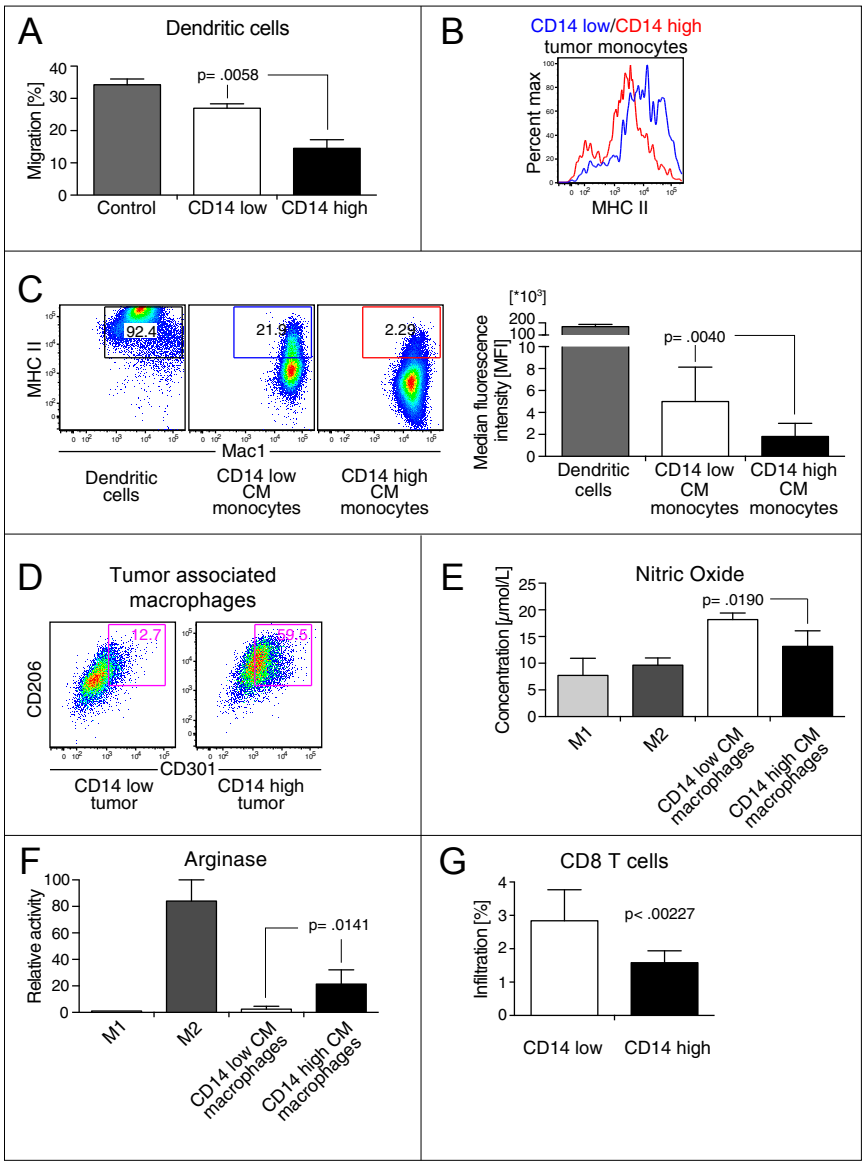

Fig. S4. CD14-high BC cells promote myeloid cell recruitment and immune suppression. (*A*) Chemotaxis of dendritic cells across a transwell in response to different tumor CMs ($n = 4$) (mean and SEM; $P = 0.0058$). (*B*) Histogram indicates MHC II expression on tumor-infiltrating monocytic cells (Gr-1+ CD11b+) from each BC subpopulation. (*C*, *Left*) Flow cytometry analysis of monocytes cultured in different tumor CMs or GM-CSF and IL4 as control for 7 d. Frequency of monocytes expressing MHC II at the end of the culture is indicated. (*Right*) Quantification of MHC II expression by median fluorescence intensity (MFI) ($n = 3$) (mean and SEM; $P = 0.0040$). (*D*) Flow cytometry analysis of TAMSs (Gr-1− CD11b+ F4/80+) in BC tumors. For each plot, the gate for CD206 and CD301 was determined based on FMO control. (*E*) Nitric oxide production by bone-marrow–derived macrophages polarized in tumor CMs followed by LPS stimulation ($n = 4$) (mean and SEM; $P = 0.0190$). (*F*) Arginase activity of bone-marrow–derived macrophages polarized in tumor CMs followed by LPS stimulation ($n = 4$) (mean and SEM; $P = 0.0141$). (*G*) Frequencies of CD8 T-cell infiltration in tumors formed by CD14-low and CD14-high MB49 subpopulations in syngeneic wild-type mice. CD8 T cells were gated based on CD45+ CD3ε+ CD90+ CD8+ cells ($n = 5$) (mean and SEM; $P = 0.0227$).

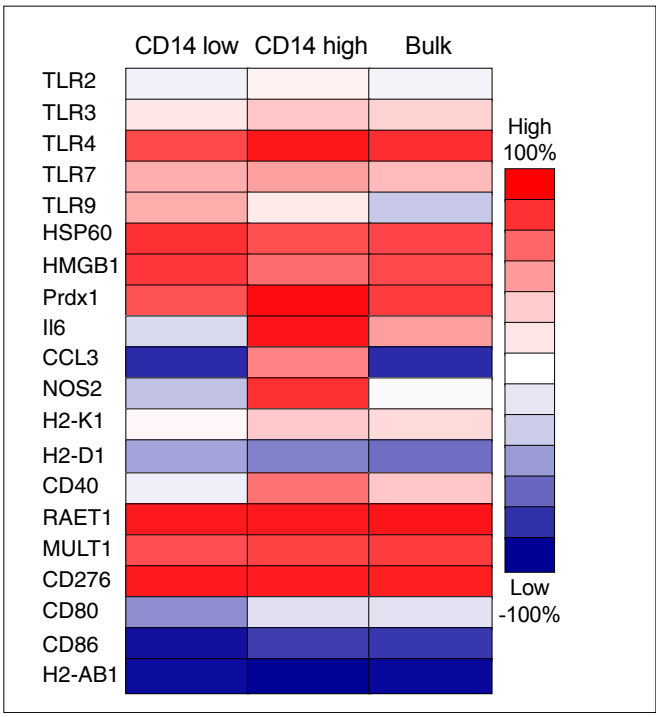

Fig. S5. A heat map of select gene expression by microarray analysis of CD14-low, CD14-high, and bulk-unsorted MB49 populations. MB49 subpopulations are in columns and genes are in rows. The color code for expression levels is to the right.

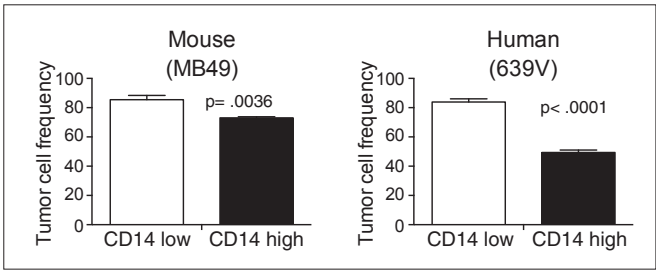

Fig. S6. CD14-high BC cells promote tumor growth by inducing proliferation of CD14-low BC cells. CD14-low and CD14-high 639V human and MB49 mouse BC subpopulations were implanted by s.c. injection into immune-compromised NSG mice. Frequency of tumor cells in the ectopic tumors was analyzed by flow cytometry and calculated based on the percentage of the indicated cell population over total live cells. MB49 tumor cells: CD45− CD44+; 639V tumor cells: H-2Kd− CD90+ ($n = 5$) (mean and SEM; MB49, $P = 0.0036$; 639V, $P < 0.0001$).